Proceedings of the 35th European Safety and Reliability & the 33rd Society for Risk Analysis Europe Conference
Edited by Eirik Bjorheim Abrahamsen, Terje Aven, Frederic Bouder, Roger Flage, Marja Ylönen
©2025 ESREL SRA-E 2025 Organizers. *Published by* Research Publishing, Singapore.
doi: 10.3850/978-981-94-3281-3_ESREL-SRA-E2025-P2809-cd

Robust Prognostics for Composite Structures Facing Unforeseen Impacts

Mariana Salinas-Camus

Intelligent Sustainable Prognostics Group, Aerospace Structures and Materials Department, Faculty of Aerospace Engineering, Delft University of Technology, Netherlands. E-mail: m.salinascamus@tudelft.nl

George Galanopoulos

Faculty of Aerospace Engineering, Delft University of Technology, Netherlands.

Ethan Jull

Defence, Safety and Security Department, TNO, Netherlands.

Lucas Amaral

Defence, Safety and Security Department, TNO, Netherlands.

Nick Eleftheroglou

Intelligent Sustainable Prognostics Group, Aerospace Structures and Materials Department, Faculty of Aerospace Engineering, Delft University of Technology, Netherlands. E-mail: n.eleftheroglou@tudelft.nl

Prognostics and Health Management (PHM) has gained prominence in recent years due to the increasing complexity of engineering systems and structures. Many of these systems lack comprehensive physical models that accurately describe their degradation processes, and there is limited engineering experience regarding their real-world operational behavior. Consequently, ensuring that predefined safety standards are met throughout the operational lifecycle has become critical. To train prognostic models, it is essential to gather data that captures the degradation process accurately. However, varying operational conditions can significantly impact degradation, underscoring the need for robust prognostic models capable of adapting to different operational scenarios and unexpected events.

This work presents a novel adaptive prognostics model, the Adaptive Hidden Semi-Markov Model (AHSMM), designed to provide reliable Remaining Useful Life (RUL) predictions for engineering systems and structures under diverse loading conditions. Specifically, acoustic emission (AE) data from glass fiber-reinforced polymer (GFRP) specimens subjected to fatigue loading were used to train the model. To assess the robustness of the AHSMM, GFRP specimens were tested under the same fatigue conditions, but with multiple impacts simulating real-world phenomena such as hail. The AHSMM demonstrated its robustness and predictive accuracy outperforming the standard Hidden Semi-Markov Model (HSMM).

Keywords: PHM, prognostics, adaptive hidden semi markov model, remaining useful life, composites

1. Introduction

Prognostics and Health Management (PHM) has become an essential component in ensuring the reliability and safety of complex engineering systems and structures. As these systems grow in complexity and operate in increasingly variable conditions, the ability to predict their Remaining Useful Life (RUL) and detect potential failures before they occur has become critical for maintaining operational safety and optimizing maintenance strategies. Many modern systems lack comprehensive physical models to describe their degradation processes accurately, particularly under diverse or unpredictable operational scenarios. Consequently, developing robust prognostic models that can adapt to different operational conditions is crucial.

Structural health monitoring (SHM), a key enabler of PHM, employs a network of sensors to monitor system degradation over time (Kessler and Spearing, 2002). SHM encompasses diagnostics, which identify and quantify damage (Khodaei and Aliabadi, 2016; Marques et al., 2019), and prognostics, which forecast the structures' future condition and RUL (Saxena et al., 2011). Prognostics is particularly challenging but essential for optimizing fleet availability and maintenance schedules.

Many modern systems lack detailed physical models, making data-driven prognostic models a suitable approach, particularly for composites (Guo et al., 2019). State-of-the-art models, such as Deep Learning (DL), Long Short-Term Memory (LSTM), and Convolutional Neural Networks (CNNs), can achieve high accuracy but are sensitive to the quality of training data, environmental uncertainties, and unforeseen events (da Costa et al., 2020; Li et al., 2020; Vollert and Theissler, 2021). This sensitivity can result in poor generalization and unreliable predictions under real-world conditions.

In contrast, unsupervised stochastic models provide a promising alternative, particularly in scenarios where labeled failure data is limited (Jouin et al., 2016). Models like the Adaptive Non-Homogeneous Hidden Semi-Markov Model (ANHHSMM) (Eleftheroglou et al., 2020) are especially valuable in real-world applications due to their ability to adapt to operational changes and unexpected phenomena providing a robust prognostic model. In addition, these models improve reliability in prognostic tasks as they inherently treat RUL as a random variable rather than a deterministic one, allowing them to account for the inherent uncertainties in prognostics.

Given the growing use of composite materials in safety-critical industries such as aerospace and automotive, developing reliable and robust methods for monitoring their degradation is essential. While much of the existing literature focuses on residual strength estimation or damage progression (Lee et al., 2022; Chiachío et al., 2014), few studies address RUL prediction (Peng et al., 2015; Wu and Yao, 2010). Prominent examples include using Non-Homogeneous Hidden Semi-Markov Models for fatigue life prediction (Eleftheroglou and Loutas, 2016) and Gaussian process regression for RUL estimation in stiffened panels (Galanopoulos et al., 2023; Eleftheroglou et al., 2024).

Although impact damage in composites is well-studied, the combined effects of impact and fatigue loading remain underexplored (Sadighi and Alderliesten, 2022).

This paper presents an Adaptive Hidden Semi-Markov Model (AHSMM) to predict the RUL of glass fiber-reinforced polymer (GFRP) specimens subjected to multiple impacts during fatigue loading. By training the model with acoustic emission (AE) data, its performance under varying and complex conditions is evaluated, demonstrating its robustness, adaptability, and predictive accuracy in real-world scenarios.

The remainder of the paper is organized as follows: Section 2 introduces the development of the AHSMM, Section 3 describes the experimental case study, Section 4 presents and discusses the results, and Section 5 concludes the paper.

2. Adaptive Hidden Semi Markov Model

The AHSMM is an improvement of the established Hidden Semi-Markov Model (HSMM) (Yu, 2010). The adaptive features of the AHSMM are inspired by the methodology presented in (Eleftheroglou et al., 2020).

The HSMM itself extends the capabilities of the Hidden Markov Model (HMM) (Rabiner, 1989) by incorporating a variable sojourn time for each damage state. This means that for each damage state, a number of observations are emitted based on the sojourn time of that damage state. In this study, the sojourn time for each damage state follows a Weibull distribution. An HSMM is defined by three main elements: the number of damage states, N; the number of distinct observation symbols, M; and the transition rate function, λ. To train the HSMM, the Expectation-Maximization (E-M) algorithm is utilized, as detailed in (Yu, 2010).

However, specific assumptions are made to make the model suitable for prognostics. First, the model always starts in the first hidden state, implying that the structure begins in a “good-as-new” condition. Second, only left-to-right transitions are permitted, meaning the structure’s health cannot recover, and all states must be traversed sequentially until failure. Lastly, the final state is observable and represents failure, emitting a single observation value.

As mentioned, the AHSMM introduces adaptivity to the HSMM. During the testing phase, adaptation is triggered whenever a transition occurs from damage state S_i to S_{i+1}. The sojourn time of state S_i, denoted T_i, is then compared to the expected value E_i derived from the training phase via the Weibull distribution for that state. The Weibull distribution is defined by two parameters, α (shape) and β (scale), as shown in Equation 1. The expected value of the distribution is given in Equation 2.

$$f(x) = \begin{cases} \frac{\alpha}{\beta}\left(\frac{x}{\beta}\right)^{\alpha-1} e^{-\left(\frac{x}{\beta}\right)^{\alpha}}, & x \geq 0, \\ 0, & x < 0. \end{cases} \tag{1}$$

$$\mathbb{E}[X] = \beta\Gamma\left(1 + \frac{1}{\alpha}\right) \tag{2}$$

A ratio between T_i and E_i of the current damage state, S_i, is calculated and used as a resampling factor (RF) for the sojourn time of the next damage state, S_{i+1}. To resample the sojourn time of S_{i+1}, the scale parameter is adapted since it can shift the Weibull distribution to have shorter and longer sojourn times. The adapted scale parameter for the damage state S_{i+1} is denoted as β^*_{i+1} and is defined in Equation 3. Thus, the Weibull distribution for S_{i+1} is defined by the parameters $(\alpha_{i+1}, \beta^*_{i+1})$ since the parameter α is not adapted and remains the same as the one calculated during the training phase.

$$\beta^*_{i+1} = \frac{E_{i+1} * RF}{\Gamma(1 + \frac{1}{\alpha_{i+1}})} \tag{3}$$

Finally, to predict the RUL a prognostic measure must be used. In this paper, a time-dependent prognostic measure is used (Salinas-Camus and Eleftheroglou, 2024). $D_i(d)$ represents the pdf (or pmf for the discrete case) evaluated in the probability of transition to the same state i. The variable τ is the time spent in the current state i. Therefore, the term $D_i(d-\tau)$ represents a shift in the pdf making this RUL expression time-dependent. The variables $d^T_{i,i+1}$ and $d^T_{i,i}$ are derived from the transition rate function.

$$\begin{aligned} RUL^t_i = d^T_{i,i}\Bigg(& D_i(d-\tau) \\ & + \sum_{k=i+1}^{N-1} D_k(d) + \mathcal{N}(1,\epsilon)\Bigg) \\ & + d^T_{i,i+1}\Bigg(\sum_{k=i+1}^{N-1} D_k(d) + \mathcal{N}(1,\epsilon)\Bigg) \end{aligned} \tag{4}$$

$$d^T_{i,i+1} = P(d \leq \tau | S_t = i) \tag{5}$$

$$d^T_{i,i} = 1 - d^T_{i,i+1} \tag{6}$$

The expression gives as output a pdf of the RUL per time step. To account for uncertainty in the predictions, the confidence intervals are calculated using the cumulative density function (CDF) with a confidence level of 95%. Since the AHSMM is a stochastic model, the uncertainty reflected in the pdf corresponds to the aleatory uncertainty with the added uncertainty propagation that comes from the prognostic measure. Aleatory uncertainty refers to the inherent variability or randomness in a system or process that cannot be reduced, even with more information or data (Salinas-Camus and Eleftheroglou, 2024).

3. Experimental campaign

3.1. *Specimen specifications and experiments*

GFRP coupons are manufactured from SL90 – T0/EGL and a 10 mm hole is drilled in the center of the coupons. The nominal coupon dimensions are 400 mm x 45 mm and an 8-ply quasi-isotropic layout of $[0/+45/90/-45]_S$ is employed, leading to a nominal thickness of 7.7 mm. A representative specimen can be seen in Figure 1. First, quasi-static tensile tests are performed to define the collapse load, which averaged at 67 kN; using a 1.5 mm/min loading rate. This value guided the selection of the load level during subsequent tensile fatigue tests.

The fatigue experiments consisted of constant amplitude tension-tension fatigue, with a fixed load at 50% of the average collapse load, an R of

Fig. 1.: GFRP coupon depiction and dimensions.

0.1, and a frequency of 4 Hz. Fatigue is carried out on an MTS hydraulic machine with a load capacity of 250 kN. Every 500 cycles, fatigue loading is paused for 2 seconds, to allow for pictures to be taken at the maximum load. In addition, acoustic emission sensors are mounted on the coupons and record continuously throughout the tests. The experimental campaign is divided into two parts, regular fatigue tests and fatigue tests with multiple impacts at various times during the test. Impacts are performed through a gas gun, and the projectile is made of aluminum, attached to a plastic cylinder that matches the radius of the barrel, weighing approximately 16 g (Figure 2).

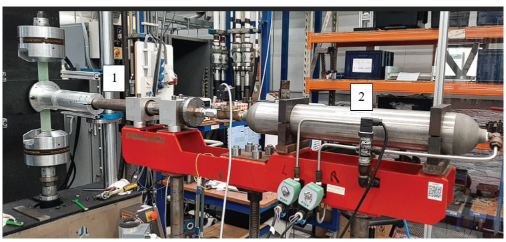

((a)) Impact gas gun setup.

((b)) Projectile.

Fig. 2.: Impact setup and projectile dimensions.

The impact(s) aims to introduce unexpected events during the coupon's degradation process —– events that typically occur during the structure's operation —– affecting its structural integrity and consequently reducing its lifetime. These impacts also serve as a challenge to assess the ability of the proposed prognostic model to capture and adapt their estimations to unexpected scenarios. The fatigue life of the pristine and impacted specimens is reported in Table 1 and Table 2 respectively. The impact(s) is performed on the hole's location (see Figure 1).

Table 1.: Unimpacted specimen fatigue lifetime.

Spec. No.	Total Cycles
6	141631
7	88371
8	66822
9	68395
10	67690
11	157758
14	139814
20	94896
22	111500
26	94120
28	112169

Table 2.: Impacted specimen information and lifetime.

Spec. No	Impact pressure (bar) x number	Time of Impact (cycles)	Total Cycles
17	1.5 x 2	5k and 10k	64313
23	1.5 x 3	5k x 3	44758

3.2. *Prognostic feature extraction*

Identifying sensitive features for RUL prognostics is crucial. Hence, the AE data collected during the tests are processed to create indices for the RUL estimation. Firstly, the low-level AE features (amplitude, duration, rise time, energy, counts, etc.) are windowed using a non-overlapping 500-cycle window. Then, 16 statistical features, such as mean, median, variance, skewness, etc., are calculated for each window for both the time and frequency domains.

In addition, principal component analysis (PCA) is performed in both domains including low-level AE features and statistical features. The PCA model, similar to (Loukopoulos et al., 2019), is created using data from the healthy state —- time of first impact or 10k cycles if no impact is performed —- and then the entire dataset is transformed to the principal component space. Then, the cumulative squared reconstruction residual (Q) and Hotelling's T2 are calculated, and a natural logarithm is applied to improve processability.

The suitability of the extracted features was evaluated using the sum of Spearman rank monotonicity (Mo) Equation 7, prognosability (Prog) Equation 8, and trendability (Tr) Equation 9 (Eleftheroglou et al., 2018).

$$\text{Mo} = \frac{1}{M}\sum_{j=1}^{M} \left|\text{corr}\left(\text{rank}(x_j), \text{rank}(t_j)\right)\right| \quad (7)$$

$$\text{Prog} = \exp\left(-\frac{\text{std}_j\left(x_j(N_j)\right)}{\text{mean}_j\left|x_j(1) - x_j(N_j)\right|}\right), \quad j = 1, \ldots, M \quad (8)$$

$$\text{Tr} = \min_{j,k}\left|\frac{\text{cov}(x_j, x_k)}{\sigma_{x_j}\sigma_{x_k}}\right|, \quad j, k = 1, \ldots, M \quad (9)$$

Among the extracted features, lnQ calculated from the frequency domain features demonstrated the best performance based on the aforementioned metrics. Its behavior is illustrated in Figure 3. This feature will be utilized as the input for training the prognostic model to predict RUL.

The dataset is divided into training and testing sets where the training data includes only unimpacted specimens, while the test data consists solely of impacted specimens. This approach aims to assess the proposed methodology's ability to handle unseen events during training, highlighting its robustness and reliability in adapting to unexpected scenarios commonly encountered during operation.

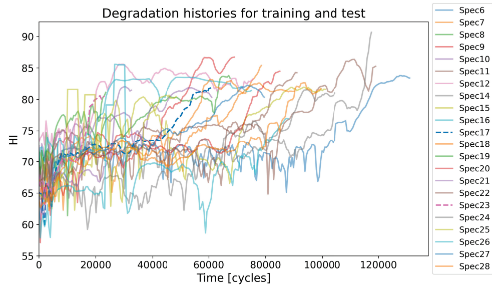

Fig. 3.: Selected feature comparison between the different specimens

4. Results and discussion

The prognostic models were trained on data from unimpacted specimens and tested on specimens subjected to multiple impacts, simulating real-world scenarios. To assess the benefits of introducing adaptivity into the prognostics framework, the AHSMM proposed in this study was compared against the standard, non-adaptive HSMM. The results, illustrated in Figure 4, and the RMSE values summarized in Table 3, highlight the superior performance of the AHSMM.

For specimen 17, the AHSMM demonstrates a clear advantage by maintaining narrower confidence intervals and a closer alignment with the true RUL trajectory throughout the specimen's lifetime. The AHSMM achieves a 55% reduction in RMSE.

Specimen 23 on the other hand, has a shorter life than any specimens used for training, given that the impacts often result in a significant lifetime reduction. Despite the reduced lifetime, the AHSMM was able to adapt effectively. Notably, after the first adaptation around cycle 20,000, the AHSMM's predictions exhibit substantial improvements in accuracy. The RMSE was reduced by 46%, reflecting the robustness of the adaptive mechanism in handling unobserved data.

A further advantage of the AHSMM lies in its ability to provide narrower confidence intervals, ensuring that the true RUL consistently falls within these bounds. This contrasts with the HSMM, whose wider confidence intervals sometimes fail to encompass the true RUL. Addition-

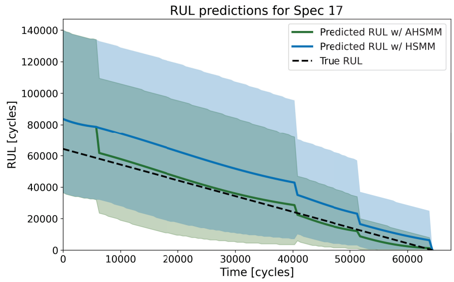

((a)) RUL predictions for specimen 17.

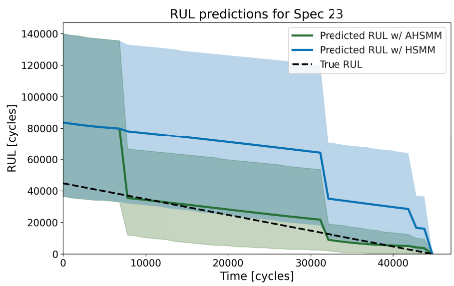

((b)) RUL predictions for specimen 23.

Fig. 4.: Comparison of RUL predictions between HSMM and AHSMM for 4(a) specimen 17 and 4(b) specimen 23.

ally, the true RUL for specimen 23 tends to lie near the lower bound of the HSMM's prediction intervals, further demonstrating its limitations.

Table 3.: RMSE value for AHSMM in the test set.

Spec. No.	HSMM (x500 cycles)	AHSMM (x500 cycles)
17	34.22	15.35
23	102.29	54.75

The predictive reliability of the AHSMM highlights its potential for practical applications where accurate prognostics are essential for decision-making and maintenance planning. The integration of adaptive mechanisms ensures that the model remains applicable across a wide range of operating conditions, making it a valuable tool for engineering systems and structural health monitoring.

5. Conclusions

This study presents an Adaptive Hidden Semi-Markov Model (AHSMM) for reliable RUL predictions of composites under fatigue loading with multiple impacts. The results highlight the model's ability to adapt to real-time degradation data and provide reliable RUL predictions even under complex and unforeseen scenarios.

By training the AHSMM on unimpacted specimens and testing it on impacted ones, the study showcased the model's remarkable robustness and reliability. The significant reduction in RMSE values highlights the critical role of online adaptation in improving prognostic accuracy. The AHSMM's ability to closely track true RUL values, particularly during the later stages of degradation, underscores its potential for practical applications in PHM.

The comparative analysis with the standard Hidden Semi-Markov Model (HSMM) further emphasized the AHSMM's robustness. The AHSMM outperformed the classical HSMM, as shown in the RUL plots. This adaptability is crucial for composites, which are often affected by operational uncertainties and environmental factors that impact their degradation.

However, the study also highlighted areas for improvement, particularly in reducing the width of the confidence intervals. While the AHSMM achieves narrower confidence intervals compared to the HSMM, they remain excessively wide, which could pose challenges for effective decision-making.

In conclusion, the AHSMM provides a reliable and robust framework for RUL prediction, making it a valuable tool for PHM applications in safety-critical industries such as aerospace. Its ability to adapt to diverse scenarios and reduce prediction errors lays a strong foundation for advancing prognostics and supporting maintenance decision-making in complex engineering systems and structures.

References

Chiachío, M., J. Chiachío, G. Rus, and J. L. Beck (2014). Predicting fatigue damage in composites: A bayesian framework. *Structural Safety 51*, 57–68.

da Costa, P. R. d. O., A. Akçay, Y. Zhang, and U. Kaymak (2020). Remaining useful lifetime prediction via deep domain adaptation. *Reliability Engineering & System Safety 195*, 106682.

Eleftheroglou, N., G. Galanopoulos, and T. Loutas (2024). Similarity learning hidden semi-markov model for adaptive prognostics of composite structures. *Reliability Engineering & System Safety 243*, 109808.

Eleftheroglou, N. and T. Loutas (2016). Fatigue damage diagnostics and prognostics of composites utilizing structural health monitoring data and stochastic processes. *Structural Health Monitoring 15*(4), 473–488.

Eleftheroglou, N., D. Zarouchas, and R. Benedictus (2020). An adaptive probabilistic data-driven methodology for prognosis of the fatigue life of composite structures. *Composite Structures 245*, 112386.

Eleftheroglou, N., D. Zarouchas, T. Loutas, R. Alderliesten, and R. Benedictus (2018). Structural health monitoring data fusion for in-situ life prognosis of composite structures. *Reliability Engineering & System Safety 178*, 40–54.

Galanopoulos, G., N. Eleftheroglou, D. Milanoski, A. Broer, D. Zarouchas, and T. Loutas (2023). A novel strain-based health indicator for the remaining useful life estimation of degrading composite structures. *Composite Structures 306*, 116579.

Guo, J., Z. Li, and M. Li (2019). A review on prognostics methods for engineering systems. *IEEE Transactions on Reliability 69*(3), 1110–1129.

Jouin, M., R. Gouriveau, D. Hissel, M.-C. Péra, and N. Zerhouni (2016). Particle filter-based prognostics: Review, discussion and perspectives. *Mechanical Systems and Signal Processing 72-73*, 2–31.

Kessler, S. S. and S. M. Spearing (2002). Design of a piezoelectric-based structural health monitoring system for damage detection in composite materials. *Smart Structures and Materials 2002: Smart Structures and Integrated Systems 4701*, 86–96.

Khodaei, Z. S. and M. H. Aliabadi (2016). A multi-level decision fusion strategy for condition based maintenance of composite structures. *Materials 9*(9).

Lee, I.-Y., H. Doh Roh, and Y.-B. Park (2022). Prognostics and health management of composite structures under multiple impacts through electromechanical behavior and a particle filter. *Materials & Design 223*, 111143.

Li, X., W. Zhang, H. Ma, Z. Luo, and X. Li (2020). Data alignments in machinery remaining useful life prediction using deep adversarial neural networks. *Knowledge-Based Systems 197*, 105843.

Loukopoulos, P., G. Zolkiewski, I. Bennett, S. Sampath, P. Pilidis, X. Li, and D. Mba (2019). Abrupt fault remaining useful life estimation using measurements from a reciprocating compressor valve failure. *Mechanical Systems and Signal Processing 121*, 359–372.

Marques, R., M. Unel, M. Yildiz, and A. Suleman (2019). Remaining useful life prediction of laminated composite materials using thermoelastic stress analysis. *Composite Structures 210*, 381–390.

Peng, T., Y. Liu, A. Saxena, and K. Goebel (2015). In-situ fatigue life prognosis for composite laminates based on stiffness degradation. *Composite Structures 132*, 155–165.

Rabiner, L. R. (1989). A tutorial on hidden markov models and selected applications in speech recognition. *Proceedings of the IEEE 77*(2), 257–286.

Sadighi, M. and R. Alderliesten (2022). Impact fatigue, multiple and repeated low-velocity impacts on frp composites: A review. *Composite Structures 297*. 4y7mi Times Cited:43 Cited References Count:142.

Salinas-Camus, M. and N. Eleftheroglou (2024). Uncertainty in aircraft turbofan engine prognostics on the c-mapss dataset. In *PHM Society European Conference*, Volume 8, pp. 10–10.

Saxena, A., K. F. Goebel, C. C. Larrosa, V. Janapati, S. Roy, and F.-K. Chang (2011). Accelerated aging experiments for prognostics of damage growth in composite materials. Technical report.

Vollert, S. and A. Theissler (2021). Challenges of machine learning-based rul prognosis: A review on nasa's c-mapss data set. In *2021 26th IEEE International Conference on Emerging Technologies and Factory Automation (ETFA)*, pp. 1–8. IEEE.

Wu, F. and W. Yao (2010). A fatigue damage model of composite materials. *International Journal of Fatigue 32*(1), 134–138.

Yu, S.-Z. (2010). Hidden semi-markov models. *Artificial Intelligence 174*(2), 215–243. Special Review Issue.